

# Carbon Nanotube Composites with Bottlebrush Elastomers for Compliant Electrodes

Jeffrey L. Self, Veronica G. Reynolds, Jacob Blankenship, Erin Mee, Jiaqi Guo, Kaitlin Albanese, Renxuan Xie, Craig J. Hawker, Javier Read de Alaniz, Michael L. Chabiny,\* and Christopher M. Bates\*



Cite This: *ACS Polym. Au* 2022, 2, 27–34



Read Online

ACCESS |



Metrics & More



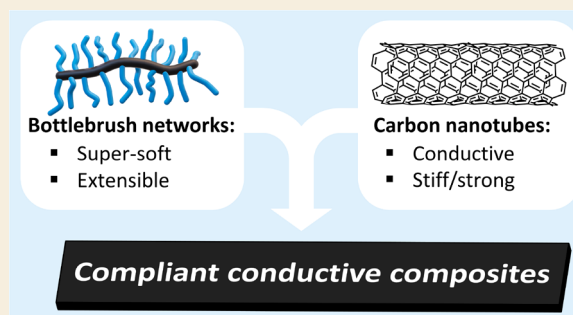
Article Recommendations



Supporting Information

**ABSTRACT:** Wearable electronics and biointerfacing technology require materials that are both compliant and conductive. The typical design strategy exploits polymer composites containing conductive particles, but the addition of a hard filler generally leads to a substantial increase in modulus that is not well-matched to biological tissue. Here, we report a new class of supersoft, conductive composites comprising carbon nanotubes (CNT) embedded in bottlebrush polymer networks. By virtue of the bottlebrush polymer architecture, these materials are several orders of magnitude softer than comparable composites in the literature involving linear polymer networks. For example, a CNT content of 0.25 wt % yields a shear modulus of 66 kPa while maintaining a typical conductivity for a CNT composite (ca.  $10^{-2}$  S/m). An added benefit of this bottlebrush matrix chemistry is the presence of dynamic polyester bonds that facilitate thermal (re)processing. This unique strategy of designing soft composites provides new opportunities to tailor the structure and properties of sustainable advanced materials.

**KEYWORDS:** bottlebrush polymer network, elastomer, composite, carbon nanotube, dynamic bonds, compliant electrode



## INTRODUCTION

Electronic devices made with soft and elastic components offer unique functionality compared to conventional, rigid silicon-based materials.<sup>1</sup> These compliant electronics have been developed for applications such as monitoring of physiological signals (e.g., electrocardiography, electroencephalography),<sup>2</sup> electronic skin for prosthetics and soft robotics,<sup>3–5</sup> and body motion tracking for injury rehabilitation and the assessment of motor control disorders.<sup>6</sup> These and other biointerfacing/mimicking devices require elastomers with electrical and mechanical properties that are atypical of conventional (insulating) rubbery networks. A variety of strategies have been developed to improve the electrical properties of elastomers by adding a second material, including blends with semiconducting polymers and composites containing conductive hard particles.<sup>7–12</sup> Carbon nanotubes (CNTs) are an ideal conductive filler due to their flexibility and high aspect ratio, which enable percolation at lower loadings than spherical particles.<sup>13</sup> However, adding any type of hard filler into a polymer presents an intrinsic challenge with respect to mechanical properties—the percolated filler network that imparts conductivity also significantly increases stiffness beyond values that are ideal for biointerfacing devices.<sup>14</sup>

A potential solution to this dichotomy lies in controlling polymer architecture. Bottlebrush polymer networks are known to be  $\sim 1$ – $2$  orders of magnitude softer than

comparable linear networks because architecture effects suppress entanglements.<sup>15</sup> This results in mechanical properties comparable to hydrogels and soft biological tissue but without the use of solvent or plasticizer.<sup>15–17</sup> Such unusually low moduli<sup>15</sup> have already been exploited to improve the performance of functional devices such as capacitive pressure sensors with enhanced sensitivity,<sup>18</sup> dielectric actuators,<sup>19</sup> and stimuli-responsive composites.<sup>20</sup> We reasoned this class of materials would also overcome current and future challenges in elastomeric conductors by maintaining a low stiffness even in the presence of conductive CNT fillers.

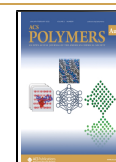
To address this opportunity, here we report a new class of supersoft (shear moduli 66–140 kPa), electrically conductive ( $1 \times 10^{-2}$ – $9 \times 10^{-2}$  S/m) bottlebrush polymer composites containing CNT fillers. In addition to excellent CNT dispersion as facilitated by a novel, solvent-free curing method, these materials include a rubbery polyester side-chain chemistry that is dynamic at elevated temperatures (180 °C). This facilitates (re)processing while also maintaining excellent

**Received:** September 16, 2021

**Revised:** October 20, 2021

**Accepted:** October 21, 2021

**Published:** November 8, 2021



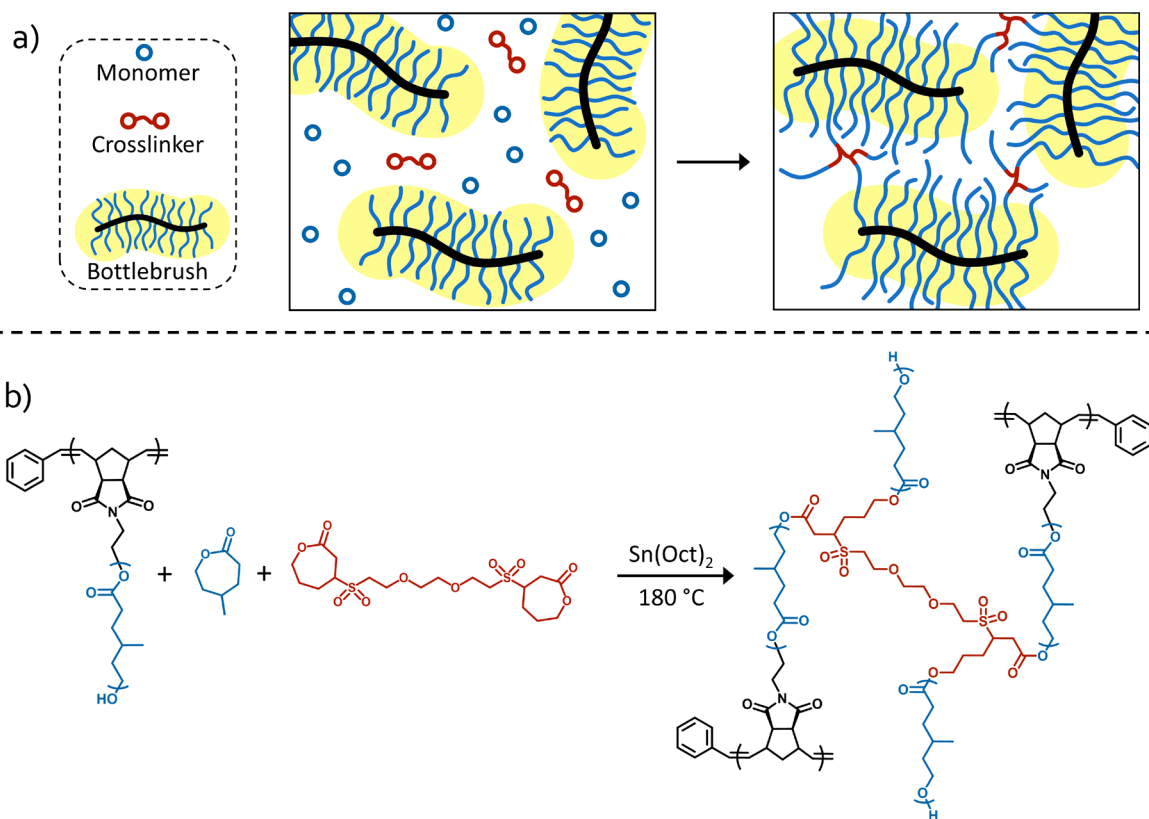


**Figure 1.** (a) Schematic representation of bottlebrush polymer network formation; note the bottlebrush polymer side chains are capable of reinitiation and complete incorporation of the monomer, which results in an all-solid material after cross-linking. (b) Chemical structures of the various resin components and the resulting bottlebrush polymer network.

mechanical integrity under ambient conditions—important attributes in sustainable device design. Collectively, these findings establish a new materials platform for conductive composites and highlight the utility of exploiting highly branched polymer architectures in advanced applications.

## RESULTS AND DISCUSSION

### Composite Design and Synthesis

Our process for forming soft, conductive composites consists of several key steps: (1) synthesizing and characterizing bottlebrush polymer precursors, (2) dispersing carbon nanotubes in a solvent-free formulation containing the bottlebrush precursor, a cross-linker, and a reactive plasticizer, and (3) curing the mixture to form all-solid elastomeric composites. Below, we detail the design and chemistry used in each step.

While there are a number of synthetic strategies available to form bottlebrush networks,<sup>21–30</sup> we selected a versatile two-step process<sup>17,18,23,29,30</sup> involving (i) the synthesis of well-defined bottlebrush precursors via “grafting-through” polymerization followed by (ii) formulation and cross-linking. As previously demonstrated, this approach allows for the rigorous characterization of bottlebrush precursors prior to cross-linking.<sup>17,18,30,31</sup>

Poly(4-methylcaprolactone) (P4MCL) was selected as the bottlebrush side-chain chemistry, since it forms robust elastomers at room temperature due to its low glass transition temperature ( $T_g \approx -60^\circ\text{C}$ ) and lack of crystallinity.<sup>17,32</sup> Two bis-telechelic P4MCL homopolymers (2.1 and 1.7 kDa, both below the reported entanglement molecular weight of 2.9 kDa<sup>33</sup>) were synthesized via ring-opening polymerization

(ROP) from a norbornene–alcohol initiator using tin ethylhexanoate ( $\text{Sn}(\text{Oct})_2$ ) as the catalyst following reported procedures.<sup>17</sup> This results in P4MCL macromonomers with a single norbornene end group that can undergo ring-opening metathesis polymerization to construct the bottlebrush backbone as well as a single hydroxy chain end. The latter serves two purposes: (1) as a reactive nucleophile for cross-linking and (2) as a source of hydroxyl units for dynamic polyester exchange reactions at elevated temperatures in the presence of a Lewis acid.<sup>17,34,35</sup>

P4MCL macromonomers were subjected to the Grubbs third-generation catalyst in various stoichiometries to synthesize bottlebrush homopolymers with different backbone ( $N_{\text{BB}}$ ) and side-chain ( $N_{\text{SC}}$ ) degrees of polymerization (see Figures S1 and S2). In principle, larger values of  $N_{\text{BB}}$  are preferable, since they yield softer networks,<sup>17,30</sup> but in the context of composites, there is a practical upper limit due to the viscosity before curing, which also increases with the bottlebrush precursor molecular weight. High- $N_{\text{BB}}$  ( $\sim 400$ ) bottlebrush polymers were too viscous to be compatible with our solvent-free, centrifugal-mixing-based CNT dispersion process (see below). Instead, we found that intermediate- $N_{\text{BB}}$  bottlebrush polymers ( $\sim 100$ ) optimally balanced the trade-off between precured viscosity and postcured softness.

Even with reduced  $N_{\text{BB}}$  values, these bottlebrush polymers have high molecular weights and viscosities, making it difficult to mix CNTs in the bulk without solvent. To facilitate mixing during CNT dispersion, we plasticized the bottlebrush polymer with 4-methylcaprolactone (4MCL) monomer. Typically, the use of a nonreactive plasticizer would be undesirable as leaching can occur over time from the final material. However,

due to the living nature of ring-opening polymerization (which was used to synthesize the macromonomer), 4MCL is incorporated directly into the bottlebrush network during thermal cross-linking by reinitiation and propagation from the hydroxyl groups at the ends of side chains or those formed after reaction with the cross-linker (shown schematically in Figure 1a and structurally in Figure 1b). This approach conveniently allows for the use of plasticizer during processing while ensuring the final material lacks residual small molecules.

To further complement this strategy, we designed a new bis-lactone-based cross-linker with improved solubility in 4MCL monomer and P4MCL bottlebrush over previous analogues (Figures S3 and S4).<sup>17,32,36</sup> The two-step synthesis enables the inclusion of a bridging chain between two caprolactone units, promoting improved solubility and reduced crystallinity. Using thiol–ene chemistry, a thiol-terminated triethylene glycol was used to tether two cyclic ketones. The thioethers generated in the first step were then oxidized to sulfones, which have far greater oxidative stability than thioethers,<sup>37</sup> while simultaneously generating the bis-lactone structure necessary to drive network formation.

### Mechanical Characterization of Polymer Networks and Composites

We first focus on the curing of neat P4MCL bottlebrush networks without CNTs to assess the efficiency of our new cross-linker. A series of formulations was prepared from a 170 kDa bottlebrush polymer ( $N_{\text{BB}} = 85$ ,  $N_{\text{SC}} = 15$ ) with varying amounts of cross-linker (0.5–3 wt %) at constant catalyst (1.5 wt %) and monomer (20 wt %) loading (see Tables S1–S4). Network formation proceeds rapidly at 180 °C, nearing complete conversion within 10 min as evidenced by *in situ* rheometry (Figure 2a); the storage ( $G'$ ) and loss ( $G''$ ) moduli quickly increase and plateau with a  $\sim 10\times$  separation that indicates robust network formation. After curing, the samples were immediately cooled to 25 °C and frequency sweeps were used to measure the rubbery plateau modulus (Figure 2b). The final materials showed low-plateau moduli from 18 to 160 kPa (values well within the range of various biological tissue<sup>38</sup>) that were easily tuned through formulation. To ensure the low moduli values were not a result of unreacted monomer plasticizing the networks, sol–gel measurements were performed in duplicate for both the 0.5 and 1 wt % cross-linker samples. The average gel fractions were found to be 86 and 94% (Table S5), respectively, indicating that the monomer introduced during processing is successfully incorporated into the networks. The lowest cross-linker loading (0.5 wt %) was selected for CNT composites to target supersoft materials.

Various strategies have been developed to improve the dispersion of CNT filler in polymer networks, which is crucial for optimizing composite properties. Examples include increasing the chemical compatibility of CNTs with a polymer matrix (e.g., CNT surface functionalization or adding surfactant/dispersant molecules) and employing aggressive mixing techniques including ultrasonication or bead milling. Here, uniform CNT dispersions were achieved by mechanically mixing CNT powder into a 150 kDa bottlebrush polymer precursor ( $N_{\text{BB}} = 88$ ,  $N_{\text{SC}} = 12$ ) plasticized by 14 wt % 4MCL monomer. To better promote shear forces and break up of CNT agglomerates, ceramic cylinders were added; see Figure S6. As evidenced by optical microscopy (Figure 3), scanning electron microscopy (Figure S7), and small-angle X-ray scattering (Figure S8), this simple mixing process yields

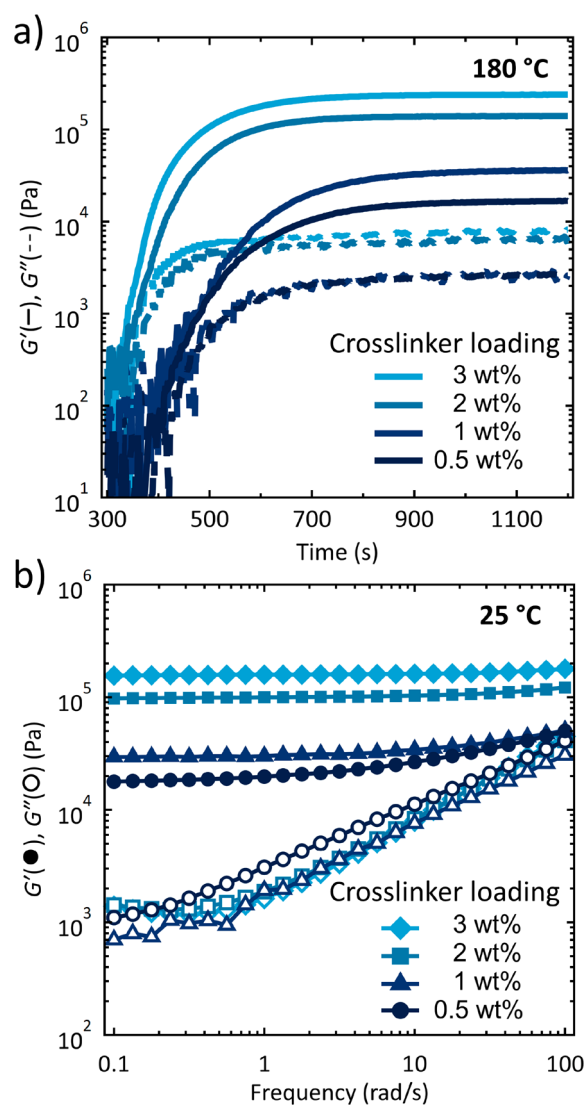


**Figure 2.** Rheological characterization of neat bottlebrush networks (no added CNTs) starting from a 170 kDa bottlebrush precursor ( $N_{\text{BB}} = 85$ ,  $N_{\text{SC}} = 15$ ). (a) *In situ* curing of various bottlebrush polymer resins truncated to highlight the region of interest; for full traces, refer to Figure S5. (b) Frequency-dependent modulus data capturing the room temperature rubbery plateau.

homogeneously dispersed CNT-doped bottlebrush polymer resins. The batch sizes in this study were approximately 1 g, which is amenable for screening various formulations and small-scale prototyping; we note that this mixing process is readily scaled up.

For the composite materials, guided by our results on unfilled formulations, a cross-linker loading of 0.5 wt % was selected to minimize the resulting sample stiffness while retaining excellent curing characteristics. The final formulation of these samples was analogous to those shown in Figure 2 but with 0.25% and 0.51% CNTs by weight (full details are provided in Tables S6–S8). Although many filler materials require substantially higher loadings to form percolating networks, the high aspect ratio of CNTs enables percolation at these low percentages.<sup>39,40</sup> Note that even prior to network formation, these samples showed characteristic elasticity induced by the presence of CNTs as observed in precuring

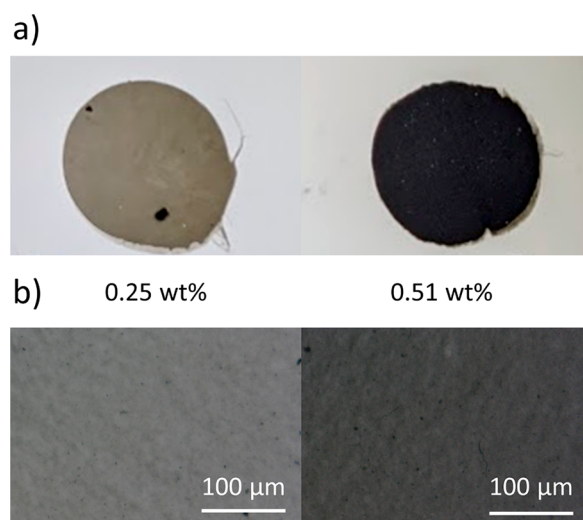


**Figure 3.** (a) Photographs of two thin films with 0.25 and 0.51 wt % CNTs after mechanical mixing. (b) Optical micrographs confirm the efficient dispersion of CNTs in P4MCL bottlebrush polymers.

frequency sweeps, which contain a rubbery plateau at low frequencies (Figure S9).

The curing traces in Figure 4a show that CNTs prevent the development of a flat plateau at long times. When heated beyond the 20 min required to cure the matrix network, composite samples exhibit a small and steady rise in modulus ( $\sim 1$  kPa/min). An effect of this magnitude would be negligible in typical composite systems where the moduli are several orders of magnitude higher, but in these soft materials ( $G' \approx 10$ – $100$  kPa), it is readily apparent. We hypothesize this secondary curing stems from reactions between the bottlebrush polymer (specifically, hydroxyl groups at the ends of side chains) and functional group defects on the CNT surface (e.g., carboxylic acids and esters).<sup>41</sup> In the absence of cross-linker and catalyst, this behavior persists (as shown in Figure S10), further indicating that side reactions between the bottlebrush polymer and CNT surface could account for the rise in modulus. Significantly, this behavior only occurs at elevated temperatures and not under ambient conditions.

When cooled to room temperature, samples with 0, 0.25, and 0.51 wt % CNTs have shear moduli ( $G'$ ) of 31, 66, and 140 kPa, respectively (as measured by rheometry, Figure 4b). Note that the 0% CNT sample is stiffer than the sample of similar composition reported in Figure 2 due to the lower molecular weight of the bottlebrush polymer precursor. Dynamic polyester–CNT composites of similar filler loading (0.25 wt % CNT) but prepared with a linear polymer reportedly have a shear modulus  $\sim 70$  MPa, nearly 3 orders of magnitude stiffer than the composites described here.<sup>42</sup> Notably, a recent report achieved a dynamic composite with a similar modulus to our materials (0.5 wt % CNT, 64 kPa) but only after 70 wt % plasticizer was added.<sup>43</sup> We caution that directly comparing the modulus of different composites can be problematic, as it is highly dependent on both the dispersion process and polymer matrix chemistry.<sup>14,39</sup> Nevertheless, our bottlebrush composites are significantly softer than others reported in the literature.

#### Electrical Properties of Bottlebrush–CNT Composites

Next, we sought to characterize the electrical impedance of our samples to understand the relationship between CNT loading

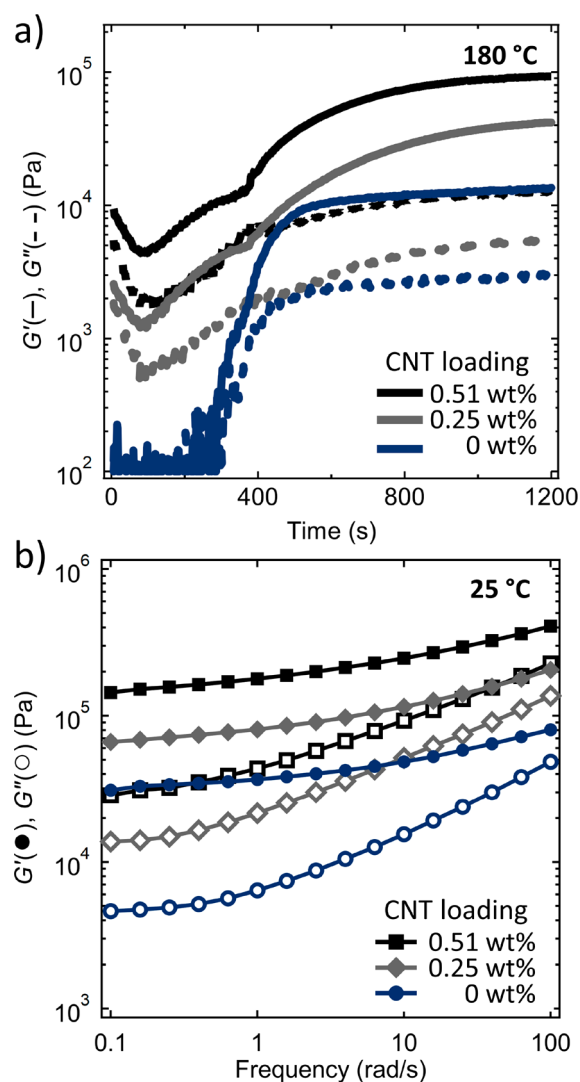


**Figure 4.** (a) Bottlebrush–CNT composites cure rapidly at 180 °C starting from a 150 kDa bottlebrush precursor ( $N_{BB} = 88$ ,  $N_{SC} = 12$ ). (b) Room temperature frequency sweeps after curing show a soft rubbery plateau.

and conductivity. The electrical properties of our bottlebrush–CNT composites were measured by AC impedance spectroscopy. Both the 0.25 and 0.51 wt % CNT composites exhibited stable conductivity across a wide frequency range (Figure 5a). Samples had frequency-independent resistance and in-phase current and voltage (typical of ideal resistors) in this frequency range, with negligible capacitance (Figure S11). The DC conductivity,  $\sigma_{DC}$ , was calculated from the plateau value of the resistance in the low-frequency limit (0.1 Hz). The 0.25 and 0.51 wt % samples had DC conductivities of  $1 \times 10^{-2}$  and  $9 \times 10^{-2}$  S/m, respectively, as shown in Table 1. Conductivity increased with CNT loading as expected, and the values were in the range of previously reported composites with similar CNT loadings (Figure S12). The measured conductivity of the composites improved with increasing DC bias, which indicates contact resistance at the electrode–elastomer interfaces (Figure S13). Therefore, the intrinsic conductivities may be higher than reported. Both composites exhibited relatively steady conductivity over time under a 4.5 V DC bias (Figure S14). To show that the composite is functional in a practical application, we used one in a simple light-emitting diode

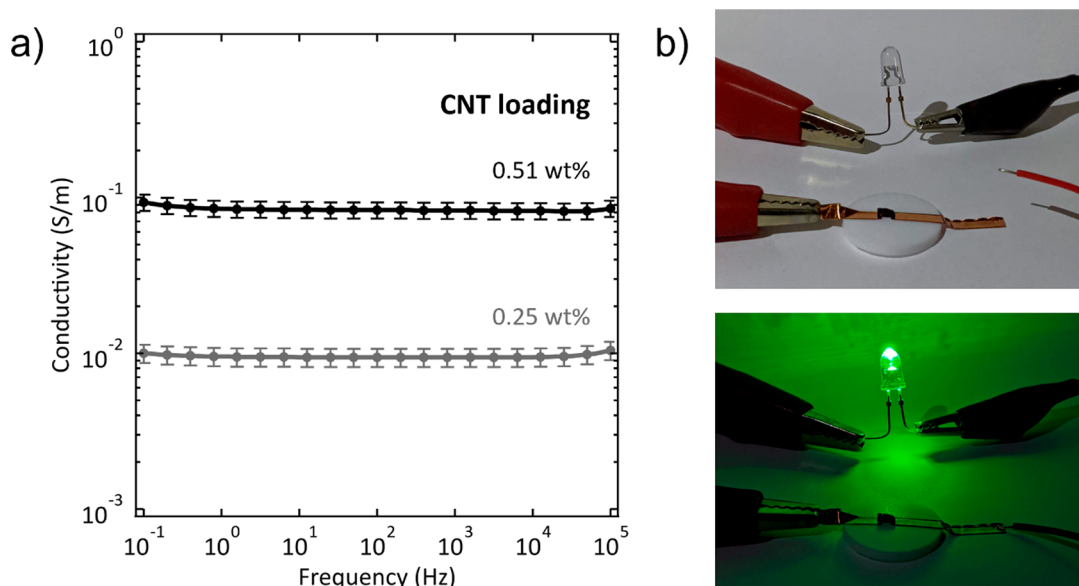


**Figure 5.** (a) Conductivity of the 0.25 and 0.51 wt % CNT composite samples measured in the frequency range of 0.1 Hz to 100 kHz (100 mV AC amplitude, no bias). (b) Photographs of the 0.51 wt % CNT sample used as a resistor to modulate the current in an LED circuit.

**Table 1. Summary of Bottlebrush–CNT Composite Properties**

CNT concentration (wt%)	shear modulus (kPa)	conductivity (S/m)
0	31	-
0.25	66	$(1 \pm 0.1) \times 10^{-2}$
0.51	140	$(9 \pm 1) \times 10^{-2}$

(LED) circuit (Figure 5b and Supplementary Movie S1). A 0.51 wt % CNT sample formed with appropriate dimensions acted as a resistor in series with a green LED and a 9 V battery; this circuit shows that device-relevant voltages can be applied to the bottlebrush–CNT composite and that DC electrical current does not lead to degradation.

### Reprocessing

Previously, polyester bottlebrush polymer networks have been shown to be dynamic and reprocessable at elevated temperatures as a result of alcohol–polyester exchange with a Lewis acid.<sup>17</sup> Unlike typical experiments used to establish dynamic covalent bond exchange, stress-relaxation measurements were

not performed at elevated temperatures on our composites given the stiffening we observed during extended heating in the presence of CNTs. Instead, to gauge whether the dynamic bottlebrush matrix can be used to facilitate reprocessing CNT composites, dynamic mechanical analysis (DMA) was used to study samples before and after compression molding (Figure 6). Two rectangular samples were fashioned; one was kept as a pristine control, while the other was cut into multiple, discrete pieces and then repressed by annealing in a mold at 180 °C for 1 h. Macroscopically, the damaged pieces reformed a cohesive solid but with greater surface roughness. The pristine sample had a tensile modulus ( $E'$ ) of 200 kPa, which agrees with the value predicted from rheometry under the assumption of elastomer incompressibility (Poisson's ratio  $\nu = 0.5$ ):  $E' = 3G' = 3(66 \text{ kPa}) = 198 \text{ kPa}$ .<sup>44</sup> In contrast, the healed sample had a significantly lower  $E' = 82 \text{ kPa}$ , indicating the material recovers approximately 40% of its original stiffness after reprocessing. Longer times or larger compression may improve this recovery, although we note in the spirit of producing soft and conductive

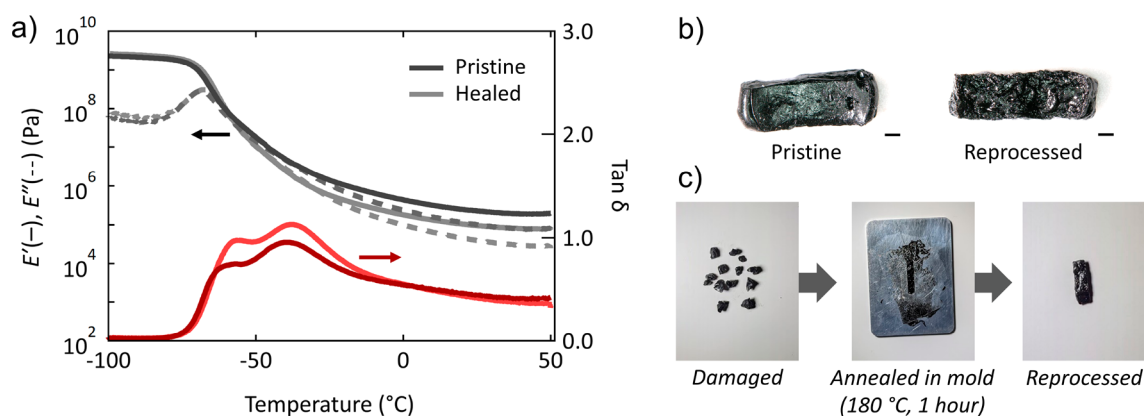


**Figure 6.** Reprocessing of a 0.25 wt % CNT bottlebrush composite with 0.5 wt % cross-linker. (a) Dynamic mechanical thermal analysis showing partial recovery of the tensile modulus (measured on cooling at 5 °C/min). (b) Optical microscopy of pristine and reprocessed samples; the scale bars are 1 mm. (c) Pictures taken throughout the process.

elastomers, it is not necessarily bad to reduce the modulus after reprocessing.

## CONCLUSIONS

In conclusion, we have developed a class of supersoft, conductive elastomers by leveraging the highly branched bottlebrush polymer architecture. Incorporating carbon nanotubes as filler particles results in composites that achieve electrical percolation at relatively low loadings (e.g., 0.25 and 0.51 wt %). Although stiffer than unfilled samples of similar composition ( $G' = 31$  kPa), the CNT composites have modulus values ( $G' = 66$  and 140 kPa) about 2 orders of magnitude smaller than analogous linear networks yet comparable conductivities ( $1 \times 10^{-2}$  and  $9 \times 10^{-2}$  S/m). We anticipate this unique combination of properties will be of use to the materials science community in applications where both softness and conductivity are valuable.

## ASSOCIATED CONTENT

### Supporting Information

The Supporting Information is available free of charge at <https://pubs.acs.org/doi/10.1021/acspolymersau.1c00034>.

Video showing a CNT sample used as a resistor to modulate the current in an LED circuit (Supplementary Movie S1) (MP4)

Reagent information, instrumentation, and synthetic methods as well as size-exclusion chromatograms and characterization of polymer samples (Figures S1 and S2), cross-linker synthesis (Figure S3 and S4), composition tables for non-CNT-containing samples (Tables S1 to S4), sol-gel data (Table S5), full curing traces of non-CNT-containing samples (Figure S5), CNT-containing network formation overview (Figure S6), scanning electron microscopy of a CNT-containing sample (Figure S7), small-angle X-ray scattering data for a CNT-containing sample (Figure S8), precuring frequency sweep data for filled samples (Figure S9), composition tables for CNT-containing samples (Tables S6 to S8), curing control of a CNT-containing sample without catalyst nor cross-linker (Figure S10), impedance and phase angle characterization (Figure S11), comparison of results with literature (Figure S12), voltage-biased conductivity data for CNT-containing samples (Figure S13), conductivity over time data for CNT-containing samples (Figure S14) (PDF)

## AUTHOR INFORMATION

### Corresponding Authors

**Michael L. Chabinyc** – *Materials Department, University of California, Santa Barbara, California 93106, United States*; [orcid.org/0000-0003-4641-3508](https://orcid.org/0000-0003-4641-3508); Email: [mchabinyc@engineering.ucsb.edu](mailto:mchabinyc@engineering.ucsb.edu)

**Christopher M. Bates** – *Materials Department, Materials Research Laboratory, and Department of Chemical Engineering, University of California, Santa Barbara, California 93106, United States*; *Department of Chemistry & Biochemistry, University of California, Santa Barbara, California 93106, United States*; [orcid.org/0000-0002-1598-794X](https://orcid.org/0000-0002-1598-794X); Email: [cbates@ucsb.edu](mailto:cbates@ucsb.edu)

## Authors

**Jeffrey L. Self** – *Department of Chemistry & Biochemistry, University of California, Santa Barbara, California 93106, United States*; [orcid.org/0000-0002-9394-4582](https://orcid.org/0000-0002-9394-4582)

**Veronica G. Reynolds** – *Materials Department, University of California, Santa Barbara, California 93106, United States*; [orcid.org/0000-0001-8356-6568](https://orcid.org/0000-0001-8356-6568)

**Jacob Blankenship** – *Department of Chemistry & Biochemistry, University of California, Santa Barbara, California 93106, United States*

**Erin Mee** – *Materials Department, University of California, Santa Barbara, California 93106, United States*

**Jiaqi Guo** – *Department of Chemical Engineering, University of California, Santa Barbara, California 93106, United States*

**Kaitlin Albanese** – *Department of Chemistry & Biochemistry, University of California, Santa Barbara, California 93106, United States*

**Renxuan Xie** – *Materials Research Laboratory, University of California, Santa Barbara, California 93106, United States*

**Craig J. Hawker** – *Department of Chemistry & Biochemistry, University of California, Santa Barbara, California 93106, United States*; *Materials Department and Materials Research Laboratory, University of California, Santa Barbara, California 93106, United States*; [orcid.org/0000-0001-9951-851X](https://orcid.org/0000-0001-9951-851X)

**Javier Read de Alaniz** – *Department of Chemistry & Biochemistry, University of California, Santa Barbara, California 93106, United States*

Complete contact information is available at:

<https://pubs.acs.org/doi/10.1021/acspolymersau.1c00034>

## Author Contributions

J.L.S., V.G.R., R.X., C.J.H., J.R.A., M.L.C., and C.M.B. designed experiments and wrote the paper. V.G.R., E.M., and J.G. performed electrical characterization, dispersion experiments, optical characterization, and conductivity demos. J.L.S., R.X., and K.A. performed rheological experiments. J.L.S. and J.B. synthesized and characterized materials.

## Notes

The authors declare the following competing financial interest(s): A provisional patent has been filed covering the results reported herein. The authors declare no other competing financial interests.

## ACKNOWLEDGMENTS

Material synthesis and characterization were supported by NSF Award No. DMR-1844987 and Award No. CMMI-2053760, respectively. J.L.S. and V.G.R. gratefully acknowledge the National Science Foundation Graduate Research Fellowship Program under Grant 1650114. Any opinions, findings, and conclusions or recommendations expressed in this material are those of the author(s) and do not necessarily reflect the views of the National Science Foundation. The research reported here made use of shared facilities of the UC Santa Barbara Materials Research Science and Engineering Center (MRSEC, NSF DMR-1720256), a member of the Materials Research Facilities Network (<http://www.mrfn.org>). Special thanks to Dr. David Goldfeld for assistance with scanning electron microscopy.

## REFERENCES

- (1) Rogers, J. A.; Someya, T.; Huang, Y. Materials and Mechanics for Stretchable Electronics. *Science* **2010**, *327* (5973), 1603–1607.
- (2) Weigel, M.; Lu, T.; Bailly, G.; Oulasvirta, A.; Majidi, C.; Steimle, J. I. *CHI '15: CHI Conference on Human Factors in Computing Systems* **2015**, 2991–3000.
- (3) Xu, S.; Zhang, Y.; Jia, L.; Mathewson, K. E.; Jang, K. I.; Kim, J.; Fu, H.; Huang, X.; Chava, P.; Wang, R.; Bhole, S.; Wang, L.; Na, Y. J.; Guan, Y.; Flavin, M.; Han, Z.; Huang, Y.; Rogers, J. A. Soft Microfluidic Assemblies of Sensors, Circuits, and Radios for the Skin. *Science* **2014**, *344* (6179), 70–74.
- (4) Shih, B.; Shah, D.; Li, J.; Thuruthel, T. G.; Park, Y.-L.; Iida, F.; Bao, Z.; Kramer-Bottiglio, R.; Tolley, M. T. Electronic Skins and Machine Learning for Intelligent Soft Robots. *Sci. Robot.* **2020**, *5* (41), No. eaaz9239.
- (5) Gomez, E. F.; Wanasinghe, S. V.; Flynn, A. E.; Dodo, O. J.; Sparks, J. L.; Baldwin, L. A.; Tabor, C. E.; Durstock, M. F.; Konkolewicz, D.; Thrasher, C. J. 3D-Printed Self-Healing Elastomers for Modular Soft Robotics. *ACS Appl. Mater. Interfaces* **2021**, *13* (24), 28870–28877.
- (6) Amit, M.; Chukoskie, L.; Skalsky, A. J.; Garudadi, H.; Ng, T. N. Flexible Pressure Sensors for Objective Assessment of Motor Disorders. *Adv. Funct. Mater.* **2020**, *30* (20), 1905241.
- (7) Xu, J.; Wang, S.; Wang, G. J. N.; Zhu, C.; Luo, S.; Jin, L.; Gu, X.; Chen, S.; Feig, V. R.; To, J. W. F.; Rondeau-Gagné, S.; Park, J.; Schroeder, B. C.; Lu, C.; Oh, J. Y.; Wang, Y.; Kim, Y. H.; Yan, H.; Sinclair, R.; Zhou, D.; Xue, G.; Murmann, B.; Linder, C.; Cai, W.; Tok, J. B. H.; Chung, J. W.; Bao, Z. Highly Stretchable Polymer Semiconductor Films through the Nanoconfinement Effect. *Science* **2017**, *355* (6320), 59–64.
- (8) Shin, M.; Oh, J. Y.; Byun, K.-E.; Lee, Y.-J.; Kim, B.; Baik, H.-K.; Park, J.-J.; Jeong, U. Polythiophene Nanofibril Bundles Surface-Embedded in Elastomer: A Route to a Highly Stretchable Active Channel Layer. *Adv. Mater.* **2015**, *27* (7), 1255–1261.
- (9) Song, E.; Kang, B.; Choi, H. H.; Sin, D. H.; Lee, H.; Lee, W. H.; Cho, K. Stretchable and Transparent Organic Semiconducting Thin Film with Conjugated Polymer Nanowires Embedded in an Elastomeric Matrix. *Adv. Electron. Mater.* **2016**, *2* (1), 1500250.
- (10) Moniruzzaman, M.; Winey, K. I. Polymer Nanocomposites Containing Carbon Nanotubes. *Macromolecules* **2006**, *39* (16), 5194–5205.
- (11) Kim, J. H.; Hwang, J. Y.; Hwang, H. R.; Kim, H. S.; Lee, J. H.; Seo, J. W.; Shin, U. S.; Lee, S. H. Simple and Cost-Effective Method of Highly Conductive and Elastic Carbon Nanotube/Polydimethylsiloxane Composite for Wearable Electronics. *Sci. Rep.* **2018**, *8* (1), 1375.
- (12) Yu, Z.; Niu, X.; Liu, Z.; Pei, Q. Intrinsically Stretchable Polymer Light-Emitting Devices Using Carbon Nanotube-Polymer Composite Electrodes. *Adv. Mater.* **2011**, *23* (34), 3989–3994.
- (13) Mutiso, R. M.; Winey, K. I. Electrical Properties of Polymer Nanocomposites Containing Rod-like Nanofillers. *Prog. Polym. Sci.* **2015**, *40* (1), 63–84.
- (14) Mensah, B.; Kim, H. G.; Lee, J.-H.; Arepalli, S.; Nah, C. Carbon Nanotube-Reinforced Elastomeric Nanocomposites: A Review. *Int. J. Smart Nano Mater.* **2015**, *6* (4), 211–238.
- (15) Daniel, W. F. M.; Burdyńska, J.; Vatankhah-Varnoosfaderani, M.; Matyjaszewski, K.; Paturej, J.; Rubinstein, M.; Dobrynin, A. V.; Sheiko, S. S. Solvent-Free, Supersoft and Superelastic Bottlebrush Melts and Networks. *Nat. Mater.* **2016**, *15* (2), 183–189.
- (16) Abbasi, M.; Faust, L.; Wilhelm, M. Comb and Bottlebrush Polymers with Superior Rheological and Mechanical Properties. *Adv. Mater.* **2019**, *31* (26), 1806484.
- (17) Self, J. L.; Sample, C. S.; Levi, A. E.; Li, K.; Xie, R.; de Alaniz, J. R.; Bates, C. M. Dynamic Bottlebrush Polymer Networks: Self-Healing in Super-Soft Materials. *J. Am. Chem. Soc.* **2020**, *142* (16), 7567–7573.
- (18) Reynolds, V. G.; Mukherjee, S.; Xie, R.; Levi, A. E.; Atassi, A.; Uchiyama, T.; Wang, H.; Chabinc, M. L.; Bates, C. M. Super-Soft Solvent-Free Bottlebrush Elastomers for Touch Sensing. *Mater. Horiz.* **2020**, *7* (1), 181–187.
- (19) Vatankhah-Varnoosfaderani, M.; Daniel, W. F. M.; Zhushma, A. P.; Li, Q.; Morgan, B. J.; Matyjaszewski, K.; Armstrong, D. P.; Spontak, R. J.; Dobrynin, A. V.; Sheiko, S. S. Bottlebrush Elastomers: A New Platform for Freestanding Electroactuation. *Adv. Mater.* **2017**, *29* (2), 1604209.
- (20) Kostrov, S. A.; Dashtimoghadam, E.; Keith, A. N.; Sheiko, S. S.; Kramarenko, E. Y. Regulating Tissue-Mimetic Mechanical Properties of Bottlebrush Elastomers by Magnetic Field. *ACS Appl. Mater. Interfaces* **2021**, *13* (32), 38783–38791.
- (21) Sarapas, J. M.; Chan, E. P.; Rettner, E. M.; Beers, K. L. Compressing and Swelling to Study the Structure of Extremely Soft Bottlebrush Networks Prepared by ROMP. *Macromolecules* **2018**, *51* (6), 2359–2366.
- (22) Vatankhah-Varnoosfaderani, M.; Daniel, W. F. M.; Everhart, M. H.; Pandya, A. A.; Liang, H.; Matyjaszewski, K.; Dobrynin, A. V.; Sheiko, S. S. Mimicking Biological Stress-Strain Behaviour with Synthetic Elastomers. *Nature* **2017**, *549* (7673), 497–501.
- (23) Arrington, K. J.; Radzinski, S. C.; Drummey, K. J.; Long, T. E.; Matson, J. B. Reversibly Cross-Linkable Bottlebrush Polymers as Pressure-Sensitive Adhesives. *ACS Appl. Mater. Interfaces* **2018**, *10* (31), 26662–26668.
- (24) Bates, C. M.; Chang, A. B.; Momčilović, N.; Jones, S. C.; Grubbs, R. H. ABA Triblock Brush Polymers: Synthesis, Self-Assembly, Conductivity, and Rheological Properties. *Macromolecules* **2015**, *48* (14), 4967–4973.
- (25) Liang, H.; Sheiko, S. S.; Dobrynin, A. V. Supersoft and Hyperelastic Polymer Networks with Brushlike Strands. *Macromolecules* **2018**, *51* (2), 638–645.
- (26) Pakula, T.; Zhang, Y.; Matyjaszewski, K.; Lee, H.; Boerner, H.; Qin, S.; Berry, G. C. Molecular Brushes as Super-Soft Elastomers. *Polymer* **2006**, *47* (20), 7198–7206.
- (27) Zhang, Y.; Costantini, N.; Mierzwa, M.; Pakula, T.; Neugebauer, D.; Matyjaszewski, K. Super Soft Elastomers as Ionic Conductors. *Polymer* **2004**, *45* (18), 6333–6339.
- (28) Choi, C.; Self, J. L.; Okayama, Y.; Levi, A. E.; Gerst, M.; Seros, J. C.; Hawker, C. J.; Read de Alaniz, J.; Bates, C. M. Light-Mediated Synthesis and Reprocessing of Dynamic Bottlebrush Elastomers under Ambient Conditions. *J. Am. Chem. Soc.* **2021**, *143* (26), 9866–9871.
- (29) Mei, H.; Mah, A. H.; Hu, Z.; Li, Y.; Terlier, T.; Stein, G. E.; Verduzco, R. Rapid Processing of Bottlebrush Coatings through UV-Induced Cross-Linking. *ACS Macro Lett.* **2020**, *9* (8), 1135–1142.
- (30) Mukherjee, S.; Xie, R.; Reynolds, V. G.; Uchiyama, T.; Levi, A. E.; Valois, E.; Wang, H.; Chabinc, M. L.; Bates, C. M. Universal Approach to Photo-Crosslink Bottlebrush Polymers. *Macromolecules* **2020**, *53* (3), 1090–1097.
- (31) Xie, R.; Mukherjee, S.; Levi, A. E.; Reynolds, V. G.; Wang, H.; Chabinc, M. L.; Bates, C. M. Room Temperature 3D Printing of Super-Soft and Solvent-Free Elastomers. *Sci. Adv.* **2020**, *6* (46), eabc6900.
- (32) Self, J. L.; Dolinski, N. D.; Zayas, M. S.; Read De Alaniz, J.; Bates, C. M. Bronsted-Acid-Catalyzed Exchange in Polyester Dynamic Covalent Networks. *ACS Macro Lett.* **2018**, *7* (7), 817–821.
- (33) Watts, A.; Kurokawa, N.; Hillmyer, M. A. Strong, Resilient, and Sustainable Aliphatic Polyester Thermoplastic Elastomers. *Biomacromolecules* **2017**, *18* (6), 1845–1854.
- (34) Brutman, J. P.; Delgado, P. A.; Hillmyer, M. A. Polylactide Vitrimers. *ACS Macro Lett.* **2014**, *3* (7), 607–610.
- (35) Montarnal, D.; Capelot, M.; Tournilhac, F.; Leibler, L. Silica-like Malleable Materials from Permanent Organic Networks. *Science* **2011**, *334* (6058), 965–968.
- (36) Wiltshire, J. T.; Qiao, G. G. Degradable Core Cross-Linked Star Polymers via Ring-Opening Polymerization. *Macromolecules* **2006**, *39* (13), 4282–4285.
- (37) Weh, R.; De Klerk, A. Thermochemistry of Sulfones Relevant to Oxidative Desulfurization. *Energy Fuels* **2017**, *31* (6), 6607–6614.

- (38) Levental, I.; Georges, P. C.; Janmey, P. A. Soft Biological Materials and Their Impact on Cell Function. *Soft Matter* **2007**, *3* (3), 299–306.
- (39) Xie, X.; Mai, Y.; Zhou, X. Dispersion and Alignment of Carbon Nanotubes in Polymer Matrix: A Review. *Mater. Sci. Eng., R* **2005**, *49* (4), 89–112.
- (40) Ponnamma, D.; Sadasivuni, K. K.; Grohens, Y.; Guo, Q.; Thomas, S. Carbon Nanotube Based Elastomer Composites-an Approach towards Multifunctional Materials. *J. Mater. Chem. C* **2014**, *2* (40), 8446–8485.
- (41) Shaffer, M. S. P.; Fan, X.; Windle, A. H. Dispersion and Packing of Carbon Nanotubes. *Carbon* **1998**, *36* (11), 1603–1612.
- (42) Yuan, D.; Guo, H.; Ke, K.; Manas-Zloczower, I. Recyclable Conductive Epoxy Composites with Segregated Filler Network Structure for EMI Shielding and Strain Sensing. *Composites, Part A* **2020**, *132*, 105837.
- (43) Zhang, G.; Patel, T.; Nallepalli, P.; Bhagat, S.; Hase, H.; Jazani, A. M.; Salzmann, I.; Ye, Z.; Oh, J. K. Macromolecularly Engineered Thermoreversible Heterogeneous Self-Healable Networks Encapsulating Reactive Multidentate Block Copolymer-Stabilized Carbon Nanotubes. *Macromol. Rapid Commun.* **2021**, *42*, 2000514.
- (44) Rubenstein, M.; Colby, R. H. *Polymer Physics (Chemistry)*, 1st ed.; Oxford University Press, 2003; p 296.